Characteristics of air showers produced by extremely high energy gamma-rays

A V Plyasheshnikov†and F A Aharonian‡

†Altai State University, Barnaul, Russia

‡ Max-Planck-Institut für Kernphysik, Heidelberg, Germany

Abstract. The technique of adjoint cascade equations has been applied to calculate the properties of air showers produced by extremely high energy (EHE) γ-rays in the energy range $10^{18} - 10^{22}$ eV. The high intrinsic accuracy, combined with very modest (compared with the traditional Monte Carlo codes) computational time requirements, make this method as an effective tool for detailed study of development of EHE showers in the Earth's atmosphere. In this paper a wide range of parameters of γ-ray induced showers are analysed taking into account two independent effects which become crucial for the cascade development in the EHE regime – the Landau-Pomeranchuk-Migdal (LPM) effect and the interaction of primary γ-rays with the geomagnetic field (GMF). Although the LPM effect leads to dramatic modifications of shower characteristics, especially at primary energies exceeding 10^{19} eV, the GMF effect, which starts to "work" approximately at same energies, prevents, to a large extent, the LPM effect by converting the primary γ-ray into a bunch of synchrotron γ-ray photons with energies effectively below the threshold of the LPM effect. This bunch of the secondary photons hits the atmosphere and creates a large number of simultaneous showers. The superposition of these independent showers mimics a single shower with energy $E = \Sigma E_{\rm i} \simeq E_0$, but without the signatures of the LPM effect. This makes the longitudinal profile of such a composite electromagnetic shower quite similar to the longitudinal profile of hadronic showers. At the same time, the number of muons as well as their lateral distribution differ significantly from the corresponding parameters of proton-induced showers. In the "gamma-ray bunch" regime, the total number of muons is less, by a factor of 5 to 10, than the number of muons in hadronic showers. Also, compared with the hadronic showers, the electromagnetic showers are characterized by a significantly narrower lateral distribution of muons. Even so, for inclined EHE γ-ray showers the density of muon flux at large distances from the shower core (≥ 1000 m) can exceed the electron density.

Short title: Characteristics of EHE gamma-ray air showers

February 1, 2008

1. Introduction

The question of the origin of most energetic particles observed in cosmic rays at energies $E \geq 10^{18}$ eV, often called Extremely High Energy cosmic rays (EHECRs), is a subject of intensive astrophysical speculations and debates. Within the conventional acceleration (or "bottom-up") scenarios, the powerful radiogalaxies, active galactic nuclei and clusters of galaxies (see e.g. [1, 2, 3]), as well as transient events like the sources of γ-ray bursts [4, 5, 6] are believed to be the most probable sites of production of EHE cosmic rays. These models have, however, a difficulty connected with the large, typically ≥ 100 Mpc distances to the most prominent representatives of these source populations. Indeed, if the observed EHE cosmic rays are protons produced in distant extragalactic sources, their interaction with the 2.7 K cosmic microwave background radiation (MBR) should give rise to the so-called Greisen-Zatsepin-Kuzmin (GZK) spectral cutoff. Depending on the characteristic distance scale to the ensemble of sources responsible for the bulk of the observed EHE cosmic ray flux, the position of the cutoff is expected between $E \sim 5 \times 10^{19}$ and 10^{20} eV (see e.g. Refs.[7, 8, 9]). Therefore, the registration of the EHECR events close to 10^{20} eV by Haverah Park, Fly's Eye, Yakutsk, and AGASA detectors (for review see Refs.[10, 11]) pose a serious challenge for any of these conventional models. This difficulty initiated a quite different approach to the solution of the problem of origin of EHE cosmic rays – the hypothesis of *non-acceleration* (or "top-down") scenario which assumes that the highest energy cosmic rays are result of decay of hypothetical massive relic particles originating from early cosmological epochs (see e.g. Ref.[12] and references therein). A distinct feature of the "top-down" models of EHECRs is an unusually high content of γ-rays with the gamma/proton ratio ≥ 1 at $E \geq 10^{20}$ eV [13, 14, 15]. Thus the gamma/proton ratio can serve as a conclusive diagnostic tool for observational proof (or rejection) of the "top-down" scenarios.

Actually, a non-negligible content of γ-rays into the EHE cosmic rays is expected also in the conventional particle acceleration models. Within these models the highest energy γ-rays are contributed through the decay of secondary π^0-mesons produced at interactions of EHECRs with 2.7 K MBR [16, 17]. If the average magnetic field in the intergalactic medium is less than 10^{-12} G, the development of the ultrarelativistic electron-photon cascades in the field of 2.7 K MBR makes the attenuation length of EHE γ-rays at $E \geq 10^{20}$ eV larger than the attenuation length of protons. Therefore, the γ-ray content in EHE cosmic ray flux depends strongly on the typical distances to the cosmic ray sources, and on the strength of the intergalactic magnetic field. It could be as large as 10 per cent in the case of homogeneous distribution of the EHECR sources in the Universe, but less than 1 per cent if the bulk of the observed EHECR flux is contributed by relatively nearby sources concentrated in our Local Supercluster

of Galaxies. Thus the measurements of the gamma/proton ratio in EHE cosmic rays by forthcoming powerful instruments like the Auger Observatory or the Telescope Array (see e.g. Ref.[10, 11]) would not only allow crucial tests to distinguish between the "top-down" and "bottom-up" scenarios, but also can provide important constraints on the spatial distribution of the EHECR accelerators within the conventional "bottom-up" models.

The effective separation of γ-ray induced showers from the proton-induced showers is possible because of noticeable differences in the development of electromagnetic and hadronic cascades. Starting from energies of about 10 TeV, the low-energy muon content becomes a reliable criterion for recognition of electromagnetic showers [18, 19, 20, 21]). At energies $E \geq 10^{16}$ eV the content of muons in the electromagnetic showers increases with an increase of energy significantly faster than in the hadronic cascades [22]. The results of this paper based on detailed numerical calculations of characteristics of electromagnetic showers, using the so-called adjoint equation technique (see for review [23]), generally confirm this effect. However, the present detailed numerical study shows that the prediction of Ref.[22] concerning the absolute muon number, based on an approximate analytical approach, was significantly overestimated.

At primary energies above 10^{19} eV the Landau-Pomeranchuk-Migdal (LPM) effect [24, 25] leads to significant suppressions of the Bethe-Heitler cross-sections for the pair-production and bremsstrahlung processes in the Earth's atmosphere, and thus dramatically changes the character of development of electromagnetic showers. In practice, however, the interesting features of electromagnetic showers caused by the LPM effect do not appear in a "pure" form, but are largely compensated by another effect connected with interactions of EHE γ-rays with the geomagnetic field (GMF) [26]. Remarkably, for the combination of relevant parameters, namely the strength and orientation of the geomagnetic field from one side, and the height, density and the mean atomic number of the Earth's atmosphere from another side, these two effects start to "operate" almost simultaneously, at energies above several times 10^{19} eV. The interaction of γ-rays with the GMF by e^+, e^- pair production does not imply, however, absorption of primary photons. In fact, the secondary (pair produced) electrons and positrons in the same geomagnetic field quickly produce a bunch of synchrotron photons with energies typically between 10^{15} and 10^{19} eV. The secondary photons initiate a large number of simultaneous electromagnetic cascades in the atmosphere. Because almost the whole energy of the primary photon is re-distributed between the synchrotron photons, the superposition of these showers mimics a single electromagnetic shower with total energy rather close to the energy of the primary particle. Moreover, because of the relatively low energies of the bunch photons, the LPM effect is essentially "switched off", and the longitudinal profile of the shower returns to the "standard" shape of electromagnetic showers without the signature of the LPM effect [22]. For typical

strengths of the GMF of about 0.2−0.6 G and for energies of primary γ-rays $E \geq 10^{20}$ eV, this interesting interference of two strong effects becomes unavoidable almost at all arrival directions of primary γ-rays. Therefore, any study of electromagnetic showers of such high energies requires thorough treatment of both the LPM and GMF effects. The depth profiles of the electronic component of EHE electromagnetic showers including these two effects have been studied by several authors [22, 27, 28, 29, 30]. Recently the characteristics of the muon component have been calculated by Capdevielle et.al. [31] using the CORSIKA Monte Carlo code. They took into account the LPM effect, but ignored the interactions of the primary γ-rays with the geomagnetic field. We generally confirm the results of these studies, but significantly extend the range of calculated characteristics. In particular, we calculated such basic parameters of electromagnetic showers as the electron size, the depth profiles of cascade particles, the content and the lateral distribution of muons and compared them with the relevant parameters of hadronic showers.

2. Interaction processes

In calculations of characteristics of electromagnetic air showers we take into account the following interaction processes – the bremsstrahlung and the ionization losses for electrons and positrons; the pair production and the Compton scattering for photons. The LPM effect [24, 25] is taken into account for the bremsstrahlung and the pair production processes. In addition, we take into consideration the interaction of EHE γ-rays with the geomagnetic field. The cross-sections of magnetic cascade processes (the pair production and the synchrotron radiation) are calculated in accordance with [32, 33].

We calculate the spatial distribution of the GMF within the framework of the dipolar central model (DCM; see e.g. [34]). In table 1 we present the GMF for two proposed sites of the Auger Observatory in Northern and Southern Hemispheres [35]. Besides the DCM results we present in table 1 the strengths of GMF obtained in Ref.[36] by use of the data of the International Geomagnetic Reference Field [37]. One can see that the dipolar central model overestimates significantly the B-field at the Southern Hemisphere site. Therefore in calculations we multiply the DCM results on B by special correction factors providing the coincidence with data of [36] near the Earth surface. With such a correction the field strength for the Northern Hemisphere site of the Auger Observatory is larger by a factor of $\simeq 2$ compared with the Southern Hemisphere site (table 1).

In figure 1 we show examples of the spatial profile of the GMF component ($B_{\rm n}$) perpendicular to the arrival direction of the air shower (note that this component of the field is the only parameter which is needed to calculate the cross-sections of both the pair-production and synchrotron processes). The parameter t in figure 1 is the distance

Table 1. The strength of the geomagnetic field (in Gauss) near the Earth surface

Site location	El Nuhuil, Mendoza (Argentina)	Millard County, Utah (USA)
Geographical coordinates	35.2^o S, 69.2^o W	39.1^o N, 112.6^o W
Observation level, g/cm^2	890	870
DCM data	0.376	0.497
Data of [36]	0.250	0.528

between the Earth surface and the observation point measured along the air shower arrival direction †. One can see that B_n increases with the zenith angle θ and decreases rapidly as a function of distance t.

For calculations of basic characteristics of photonuclear interactions of γ-rays we performed special simulations with use of the SOPHIA generator [38]. This generator provides a comprehensive tool for simulations of photohadronic processes. In particular, this code includes the excitation and decay of baryon resonances, the direct production of pions and the multiple production of hadrons. To simplify the calculation technique we assumed that all unstable particles generated in the photoproduction process (except for muons) immediately decay at the point of their generation, i.e. we neglect the finiteness of life time of such particles †. In this approximation all secondary muons are assumed to be emitted at the point of the primary γ-ray interaction. Thus, the inclusive differential (over the muon kinetic energy (T) and the muon emission angle (ϑ)) cross-section $w_\mu(E_\gamma, T, \vartheta)$ becomes the only input parameter. This cross-section is normalized as:

$$2\pi \int d\vartheta \sin\vartheta \int w_\mu(E_\gamma, T, \vartheta) dT = \sigma_{\rm ph} \cdot \bar{n}_\mu \qquad (1)$$

where σ_{ph} is the total cross-section of photoproduction, $\bar{n}_\mu$ – the mean multiplicity of muons. Following to recommendations of [18] we define the quantity $\sigma_{\rm ph}$ as $\sigma_{\rm ph} = \sigma_{\gamma \rm p} \cdot A^{0.91}$ where $\sigma_{\gamma \rm p}$ is the total cross-section of γ-ray - proton interaction (we use for this quantity data from [38]), A is the mean atomic number of air nuclei.

Besides the electromagnetic cascades we have calculated also the characteristics of proton-induced showers. A standard quark-gluon-string (QGS) model is applied in this case to describe the hadronic interactions [39, 40].

† Note that for inclined showers the B-field depends also on the azimuth angle. However, for simplicity, for such showers we assume a fixed azimuth angle corresponding to the arrival direction from the nearest geomagnetic pole.

† Our calculations show that this is a quite acceptable assumption, if one deals with muon detectors with sufficiently small threshold energy, ≤ 1 GeV.

3. Technique of adjoint cascade equations

The calculations presented below are obtained with the help of numerical solution of the adjoint cascade equations. In this section we describe shortly the main features of these equations‡.

Let us consider as an example the system of adjoint equations that describe the longitudinal development of the electromagnetic cascade. Studying the longitudinal development of such a cascade one can neglect the lateral displacement of secondary particles and their angular distribution induced mainly by the multiple Coulomb scattering. The equation system has in this case the following form

$$\lambda_e \frac{\partial f}{\partial t} + f - \int_{E_0}^{E} w_{ee}(E,E') f(t,E') dE' - \int_{E_0}^{E} w_{e\gamma}(E,E') g(t,E') dE' = \lambda_e F, \quad (2)$$

$$\lambda_\gamma \frac{\partial g}{\partial t} + g - \int_{E_0}^{E} w_{\gamma e}(E,E') f(t,E') dE' - \int_{E_0}^{E} w_{\gamma\gamma}(E,E') g(t,E') dE' = \lambda_\gamma G. \quad (3)$$

The adjoint functions f and g in Eqs. (2), and (3) describe the contributions (averaged over random realizations of the cascade development) to the response of some detector from a cascade generated by a primary electron (f) or a photon (g) of energy E; t is the distance between the observation level and a point of the primary particle appearance (measured along the particle arrival direction); E_0 is the particle detector threshold energy; λ_α is the mean free pathlength for the cascade particle of type α ($\alpha = e$ or γ); functions $w_{\alpha\beta}(E,E')$ define the differential (over the energy E') spectra of secondary particles of type β ($\beta = e$ or γ).

Properties of the detector are defined in Eqs. (2) and (3) by the right hand side functions F and G and the boundary conditions $f(t=0,E)$ and $g(t=0,E)$. For example, if the detector measures at the observation level the total number of cascade electrons with energy $E \geq E_0$, then

$$F(t,E) \equiv G(t,E) \equiv 0; \quad f(t=0,E) = H(E-E_0), \quad g(t=0,E) \equiv 0 \quad (4)$$

where $H(x) \equiv 1$ for $x \geq 0$ and $H(x) \equiv 0$ for $x < 0$.

In the case of calculation of characteristics of muons produced in the electromagnetic cascade due to nuclear interactions of cascade photons one can use a system of adjoint equations similar to Eqs. (2) and (3), but having the different form of right hand side terms and boundary conditions. For example, if the detector registers the muons transversing a circle of a given radius (R_0) with the centre at the shower axis and orientated perpendicularly to this axis, we have

$$f(t=0,E) = g(t=0,E) = 0, \qquad F(t,E) = 0, \quad (5)$$

‡ More detailed description of the adjoint equation technique is presented in [23].

$$G(t,E) = 2\pi n_0 \int d\vartheta \sin\vartheta \int w_\mu(E,T,\vartheta) p_{\rm d}(T,\vartheta) p_{\rm m}(T,\vartheta) H(\tilde{T}-T_{\rm th}) dT \ , \quad (6)$$

where w_μ is the differential cross-section of muon photoproduction defined in section 2, $T_{\rm th} = E_0 - m_\mu c^2$ – the detector threshold kinetic energy, n_0 – the concentration of air nuclei. The function

$$p_{\rm d}(T) = \exp\{-\cos\vartheta^{-1} \int_{\tilde{T}}^{T} [\lambda_{\rm dec}(T') \cdot \epsilon(T')]^{-1} dT'\} \quad (7)$$

defines the probability for the muon to survive on the way from its production point to the observation level. $\tilde{T}$ is the energy of the muon at the observation level found from the following equation

$$t/\cos\vartheta = \int_{\tilde{T}}^{T} dT'/\epsilon(T') \ , \quad (8)$$

ϵ is the ionization loss rate, and $\lambda_{\rm dec}$ is the decay mean free pathlength.

The function $p_{\rm m}$ is the probability of the muon to escape from the circle due to the multiple (Coulomb) scattering. We calculate this function using the expression for the probability distribution function of muon lateral displacements based on the solution of a special kind of the adjoint transport equation obtained by [41].

For solution of adjoint cascade equations we use a numerical method which is described in [42]. This method has been applied to solve a wide range of problems connected with cosmic ray physics (see for review [23]). The method [42] provides an accuracy of solution of adjoint equations better than a few per cent and gives results for an arbitrary region $(E_0, E_{\rm max})$ of the primary energy in *one run* of calculations. The computational time consumed by the method is quite small and depends weakly (logarithmically) on the primary energy. For example, to calculate the number of cascade electrons (or photons) for a fixed altitude of the observation level and the primary energy range $(10^9, 10^{22})$ eV one needs only a few minutes of the 1 GHz IBM PC computational time.

The results for proton-induced air showers also have been obtained by solution of adjoint cascade equations with the help of the numerical method developed in Ref. [42]. Here we do not present the expressions for these equations, because they are quite similar to Eqs. (2) and (3). They can be found in [23].

4. Comparison with previous works

A number of comparisons of air shower characteristics with similar results of previous studies has been performed to test the computational code. In figure 2 the cascade curves of photons are presented for the γ-ray induced showers developing in the homogeneous magnetic field (without presence of matter). One can see a perfect agreement with calculations of A.Goncharov [27].

Figure 3 represents the cascade curves of electrons for air showers initiated by primary γ-rays of energy 10^{20} eV, taking into account interactions with the geomagnetic field and the LPM effect. Three different combinations of the GMF and LPM effects are shown by curves 1 (no LPM, no GMF), 2 (only LPM), 3 (both LPM and GMF). A quite satisfactory agreement with the results of Ref. [22] is seen for all 3 cases.

In table 2 we present the number of muons at the sea level versus the total number of electrons for air showers created by primary γ-rays with energy below 10^{16} eV ($N_{\rm e} \leq 10^7$). Our results are compared with similar results of Edwards et.al. [19]. Note that the calculations of Ref. [19], as well as many other studies in this energy region, were performed using simplified treatments of photohadronic interactions. Namely, it was assumed that the γ-hadron interaction is identical to the inelastic interaction of the pion of the same energy. Nevertheless, a quite satisfactory agreement is seen between results presented in the table.

Table 2. The number of muons with energy $T \geq 1$ GeV as a function of the total number of electrons at the sea level for air showers created by inclined γ-rays with zenith angle 25°

.

N_e	10^5	$3 \cdot 10^5$	10^6	$3 \cdot 10^6$	10^7
N_μ, present study	$0.29 \cdot 10^3$	$0.77 \cdot 10^3$	$0.20 \cdot 10^4$	$0.51 \cdot 10^4$	$0.15 \cdot 10^5$
N_μ, [19]	$0.33 \cdot 10^3$	$0.92 \cdot 10^3$	$0.27 \cdot 10^4$	$0.65 \cdot 10^4$	$0.16 \cdot 10^5$

In table 3 we present the calculation results for the number of photoproduced muons with kinetic energy $T \geq 0$. For comparison we show also the results of calculations performed by us using the CORSIKA code [45]. It should be noted that the results in table 3 correspond to a limited primary energy region which allows us to use the CORSIKA option based on the "complete" Monte Carlo method, i.e. without the application of the "thinning technique" [46]. It is seen that discrepancy of results presented in the table does not exceed 20 %.

The "complete" Monte Carlo method requires a very large computational time which does not allow extension of simulation to extremely high energy region. To reduce the computational time one has to apply the "thinning technique" [46]. Such calculations were performed by Capdevielle et al. [31] using the same CORSIKA simulation code for EHE primary γ-rays. In table 4 we compare our results on the muon content in EHE γ-ray induced showers with similar results of Ref. [31]. Note that Capdevielle et al. [31] included in their calculations the LPM effect but ignored the effect of interactions of γ-rays with the geomagnetic field. Therefore in table 4 we show our results without the GMF effect as well. The results are in good agreement within 10 %.

Table 3. The muon content in air showers created by primary γ-rays for $z_{\rm obs}$ =890 g/cm^2. Results of the numerical solution of adjoint equations are compared with simulation results obtained by the CORSIKA code.

Primary energy of air shower, eV	$3\cdot10^{13}$	10^{14}	$3\cdot10^{14}$	10^{14}	$3\cdot10^{14}$
Zenith angle of arriving γ-ray, degree	0	0	0	45	45
N_μ, solution of adjoint equations	13.9	56.4	199	21.9	69.8
N_μ, simulations with CORSIKA	11.6	50.2	174	26.1	79.0

In figure 4 we present the radial distributions of the photoproduced muons for vertical air showers created by γ-rays with energy 10^{15} eV. Results of the numerical solution of adjoint equations are compared with the simulations made by the "complete" Monte Carlo method using the CORSIKA code. †. A perfect agreement of the results is achieved.

Table 4. The number of muons with energy $T \geq 0$ as a function of energy of the primary γ-ray for inclined (45^o) air showers. The LPM effect is included, the geomagnetic field is disabled.

E_γ, eV	10^{17}	10^{18}	10^{19}	10^{20}
N_μ, present study	$4.5\cdot10^4$	$6.1\cdot10^5$	$8.2\cdot10^6$	$7.5\cdot10^7$
N_μ, [31]	$5.0\cdot10^4$	$6.6\cdot10^5$	$8.1\cdot10^6$	$7.9\cdot10^7$

In figure 5 we present the electron cascade curves for proton induced air showers. It is seen that our results are in agreement within 20 % with simulations performed in the framework of the QGS model [44].

Table 5. The number of muons with energy $T \geq 0$ for vertical air showers created by primary protons. Z_{obs} =920 g/cm^2.

E_p, eV	10^{18}	$3\cdot10^{18}$	10^{19}	$3\cdot10^{19}$	10^{20}
N_μ, present study	$0.71\cdot10^7$	$0.19\cdot10^8$	$0.56\cdot10^8$	$0.15\cdot10^9$	$0.43\cdot10^9$
N_μ, [47]	$0.68\cdot10^7$	$0.20\cdot10^8$	$0.51\cdot10^8$	$0.16\cdot10^9$	$0.45\cdot10^9$

In table 5 we present the muon content in air showers initiated by vertical protons. Our results on this quantity are compared with similar results of Nagano et.al. [47]

† The "thinning technique" [46] does not allow adequate calculations of the radial distributions of muons in EHE electromagnetic air showers (see section 6), therefore the comparison presented in the table is limited by the primary energy 10^{15} eV.

obtained by the CORSIKA simulation code with use of the QGSJET generator of hadron interactions. The difference between these two methods does not exceed 10 %.

5. Longitudinal development of air showers

5.1. Muon component of γ-induced air showers

In the energy region below $\simeq 10^{16}$ eV the muon content in electromagnetic air showers has been studied by many authors (see e.g. [18, 19, 20, 21, 48, 49]). However, the calculations , performed in this energy region, are based, as a rule, on rather simplified treatments of the photoproduction process. For example, it was often assumed that the γ-hadron interactions were identical to the inelastic pion interactions. Recently the photohadronic interactions have been implemented into the simulation codes CORSIKA [45] and AIRES [50] allowing accurate calculations of characteristics of muons in EHE electromagnetic air showers [31, 36, 51]. However, the interaction with the geomagnetic field has not yet been included in these codes. The latter reduces essentially the applicability of calculation results on the content of photoproduced muons calculated with the help of these codes. In the present study we calculate the shower characteristics using the technique of adjoint cascade equations and considering interactions of primary γ-rays with a composite target consisting of two parts - the geomagnetic field and the Earth's atmosphere.

In figure 6 we present the dependences of the total number of muons (N_μ) at the observation level on the energy of primary γ-ray for vertical and inclined showers and for different assumptions about the LPM effect and the geomagnetic field. The following conclusions can be obtained from this figure.

- If one uses the Bethe-Heitler's cross-sections for high energy interactions of cascade particles, the energy dependence of N_μ is close to the power law, i.e. $N_\mu \sim E_\gamma^\beta$ with $\beta \simeq 0.9 - 1.0$.
- The LPM effect changes dramatically the energy dependence of N_μ. The growth of $N_\mu(E_\gamma)$ becomes less rapid; moreover a local maximum arises near $E_\gamma \simeq 10^{20} - 10^{21}$ eV, after which N_μ decreases with E_γ (curves "2" in figures 6a and 6b).
- The GMF (without the LPM effect) does not essentially change the energy dependence of $N_\mu(E_\gamma)$. It remains to be continuously growing for both the vertical and inclined showers.
- After including of the interactions with the geomagnetic field, the LPM effect does not affect considerably the $N_\mu(E_\gamma)$ dependence. However, some deviation from the power law takes place in the energy region $10^{19} \div 10^{21}$ eV. This deviation is connected with the fact, the LPM effects becomes effective a bit earlier (i.e. at

lower energies) compared with the GMF effect.

- Behaviour of $N_\mu(E_\gamma)$ for inclined air showers is generally similar to the one of the vertical showers. However, a local maximum of $N_\mu(E_\gamma)$ dependence, connected with the LPM effect, is observed for larger primary energies. Besides, for inclined showers the simultaneous influence of the LPM effect and the GMF can lead to a slight reduction of N_μ in the high energy region, whereas for vertical air showers these effects lead to a growth of N_μ.

The GMF influence on N_μ as well as on other shower characteristics has a simple explanation. For sufficiently high product $E_\gamma \cdot B_\mathrm{n}$ the primary γ-ray cannot freely enter the Earth's atmosphere due to the pair production in the geomagnetic field. The secondary (pair-produced) electrons and positrons immediately interact with the same field through the synchrotron radiation. The free pathlength of these electrons is rather small (see figure 7) compared with the scale of the magnetosphere, and weakly depends on the particle energy. Thus, these electrons emit on their way to the Earth a large number of relatively low energy photons (according to figure 7 – one photon per every 10-100 km of the trajectory). On the other hand, the mean free pathlength for the pair production grows very rapidly with reduction of the photon energy (see figure 7). As a result, the energy of primary γ-ray is distributed among a large number of secondary photons with relatively small energies not able to interact effectively with the geomagnetic field (this effect is illustrated by table 6). Thus, instead of a single γ-ray photon we have at the upper border of the atmosphere a 'bunch' of low energy photons ($E \leq 10^{19}$ eV) which thus appears below the effective threshold of the LPM effect.

Table 6. The mean number of cascade synchrotron photons produced in GMF by a vertical primary γ-ray of energy 10^{21} eV, and entering the Earth's atmosphere with energy greater than E_th.

E_{th}, eV	10^{17}	10^{18}	10^{19}
N_γ	430	135	28

In figure 8 we present the integral energy spectra of photoproduced muons. These spectra correspond to different values of the energy and arrival direction of primary γ-ray. It is seen that for vertical air showers the spectrum is rather soft; only $\simeq$30% of muons have at the observation level kinetic energy exceeding 1 GeV. However, at large arrival angles the spectrum becomes considerably flatter. For example, for $\theta = 45^\circ$ about 40-45% of muons have energy larger than 1 GeV. At the same time, the energy spectrum of photoproduced muons rather weakly depends on the primary energy.

In order to study the relation between the numbers of electrons and muons we

present in figure 9 the energy dependence of the ratio N_μ/N_e for different arrival directions. It is seen that for vertical showers the total number of muons at the observation level is very small compared with the number of electrons. Both N_e and N_μ decrease with θ, but N_e decreases faster. Thus at large zenith angles ($\theta \geq 65^\circ$) the number of muons becomes comparable or even can exceed the number of electrons.

5.2. Comparison of muon content for air showers of different nature

In figure 10 we present the energy dependence of the total number N_μ of muons for vertical showers initiated by primary γ-rays and protons. The results of the present study are compared here with results for primary γ-rays obtained in Ref. [22] using an approximate analytical solution of cascade equations, and with the results of Ref. [43, 52] for a primary proton obtained by the Monte Carlo method. On the basis of comparison of data of Ref. [22] and Ref. [43] a conclusion has been made in Ref. [22] that for EHE air showers the quantity N_μ for γ-primary can be comparable with the number of muons in proton air showers. It is seen from figure 10 that the results of present calculations on N_μ for γ-primary (curve 1) are by a factor of a few smaller than analytical results of [22] (curve 2). This discrepancy is explained by usage in Ref. [22] of a simplified model of the photoproduction process. It was assumed that the mean number of charged pions created in one γ-nuclear interaction did not depend on the γ-ray energy (E_γ) and was equal to 2. Furthermore, the energy of each of these pions was assumed to be uniformly distributed in the interval $(0,E_\gamma)$. This implies a very hard spectrum of secondary muons and an effective muon multiplicity of about 2. In fact, the multiplicity of the muons with the total energy more than 0.3 GeV † approaches to 2 only for parent γ-rays with energy equal to several GeV. It is demonstrated in figure 12 obtained using the SOPHIA generator [38]. On the other hand, the bulk of muons are produced in the electromagnetic air shower by cascade photons with typical energy of about 1 GeV for which the muon multiplicity is significantly less, $\bar{n}_\mu \simeq 0.5$ (see figure 12). At the same time, for determination of the ratio of muon contents in γ- and proton induced showers, Aharonian et al. [22] used the calculations of McComb et al. [43]. As it is seen from figure 10, the calculations of ref. [43] (curve 5) in fact predict significantly smaller number of muons compared with our calculations (curve 3). Thus, the present study does not confirm the conclusion of Ref. [22] concerning the very high ratio of $N_\mu^{(\gamma)}/N_\mu^{(p)}$.

In figure 13 we present the calculation results on the energy dependence of the ratio $\delta = N_\mu^{(\gamma)}/N_\mu^{(p)}$. One can see that this dependence has a non-trivial form. The behaviour of δ can be explained by the fact the LPM effect starts "to operate" a bit earlier than the GMF does. In the energy region above 10^{18} eV the ratio δ ranges within $\simeq 0.1 \div 0.2$.

† Exactly this value of the muon threshold energy is considered in figure 10.

In the energy region below 10^{18} eV it decreases rapidly with reduction of the primary energy in accordance with the prediction of Ref. [22].

5.3. Electron component

In figure 13 the dependence of the number of electrons on the energy of primary γ-ray is shown for the El Nuhuil site with use of different assumptions about the LPM effect and the geomagnetic field. One can see that the peculiarities of behaviour of N_e are similar to the energy dependence of the muon content described in section 5.1 (compare figures 6 and 13).

In figure 14 we show the results of calculations for the cascade curves of electrons. Such curves can be used for an approximate description of the temporal profile of the fluorescent radiation of air showers. In the case of γ-ray primary we show the cascade curves corresponding to both Northern and Southern Hemisphere sites of the Auger observatory. No significant difference between the shower profiles corresponding to γ-ray and proton induced showers can be seen. The difference in the GMF strength between Northern and Southern site locations (see table 1 and figure 1) does not affect considerably the shower profile as well. In this regard, an effective separation of γ-ray and proton-induced showers on the basis of the shower profiles seems to be hard. Perhaps such a separation could be achieved exploiting differences in the intrinsic fluctuations of the fluorescent light intensity, because the fluctuations in electromagnetic showers are smaller than in the hadronic ones (see e.g. [53]). The electromagnetic showers in the "photon bunch" regime caused by the GMF effect lead to an additional reduction of intrinsic fluctuations and, therefore, may improve the γ-ray separation efficiency.

6. Lateral distribution of photoproduced muons

No detailed studies have been done until now on the lateral distribution function (LDF) of muons in electromagnetic EHE air showers. Recently, Capdevielle et al. [31] published LDF of muons using the CORSIKA code and taking into account the LPM effect. However, they ignored the effect of interactions of γ-rays with GMF, which significantly reduces the applicability of these results. Moreover, the "thinning technique" used by these authors does not provide an acceptable accuracy of calculations for the LDF of muons.

The thinning technique has been introduced by Hillas [46]. It allows a "complete" simulation only for a high energy part of the cascade which contains secondary particles with energy larger than a fixed threshold value $E_{\rm th}$. For low energy interactions, i.e. in the energy region $\leq E_{\rm th}$, an artificial absorption of secondary particles is introduced. It is assumed that only one secondary particle survives in each interaction. For compensation of this "disappearance" of particles one should introduce appropriate statistical weights.

To avoid large fluctuations of these weights (dramatically worsening the accuracy of calculations), it is necessary to keep the thinning parameter $\epsilon = E_{th}/E$ to be sufficiently small (E is the energy of the primary particle) . The computational time needed for simulation of one air shower by this technique is approximately proportional to ϵ^{-1}.

The simulations of [31] include the LDF of photoproduced muons for 10 individual γ-ray induced air showers with primary energy 10^{20} eV. These results correspond to the value of thinning parameter $\epsilon = 10^{-6}$. For such value of ϵ one needs approximately one hour of the computational time of 500 MHz IBM PC to simulate one air shower [45]. It is seen from figure 7 of Ref. [31] that fluctuations caused by introduction of statistical weights are extremely large (up to a factor of 30). Therefore to provide an acceptably small statistical error (for example, 10%) one has to simulate an extremely large (up to $\simeq 10^5$) number of air showers. Correspondingly, this requires a great deal of the computational time. For comparison, the calculation of LDF of photoproduced muons based on the numerical solution of adjoint cascade equations is not laborious and requires less than 1 hour of the computational time. Besides, this method gives a set of LDF in an arbitrary energy region of primaries just for *one run* of calculations. Note also that this method does not contain, by definition, statistical error at all.

In figures 15, 16 we present the normalized LDF of muons of all energies, i.e. with kinetic energy $T \geq T_{th} = 0$. We define this parameter as $f_\mu(r) = \rho_\mu(r)/N_\mu$, where $\rho_\mu(r)$ is the density of the muon flux at distance r from the shower axis. Results of figure 15 correspond to different assumptions about the GMF and the LPM effects, whereas figure 16 illustrates dependence of the LDF shape on the primary energy. It is seen that the geomagnetic field only slightly modifies the LDF shape. The interaction of γ-rays with the GMF makes the LDF shape insensitive to the LPM effect. Also, the LDF only slightly depends on the primary energy (see figure 16). For example, an increase of E_γ by a factor of 10 changes the LDF no more than $\simeq$20%. On the contrary, at the absence of GMF the LPM effect would steepen considerably the shape of LDF, and make it strongly dependent on the primary energy (figure 15).

In figure 17 we present the muon density for vertical proton and γ-ray induced showers. We compare in this figure our results for primary γ-ray with the results for primary protons obtained in Ref. [47] by simulations with CORSIKA. One can see that the γ-induced shower provides an essentially narrower lateral distribution of muons compared with the proton shower. As a result, the ratio $\Delta = \rho_\mu^{(\gamma)}/\rho_\mu^{(p)}$ decreases rapidly with a growth of the radius (from $\Delta \sim 0.1$ at $r = 200$ m to $\Delta \sim 0.01$ at $r = 2500$ m). This feature of Δ can provide an effective separation of γ-induced air showers by the Auger Observatory, for which the distance from the core of the shower to the most of triggered detectors is very large, several hundred meters or more.

In figure 18 we illustrate dependence of muon LDF on the arrival direction of the

shower†. One can see that the width of the LDF increases rapidly with a growth of the zenith angle θ. This feature of LDF provides a significant contribution of the photoproduced muons to the total number of charged particles at large distances from the shower core. This effect of inclined showers is demonstrated in figure 19, where we present the particle density for two kinds of secondaries - muons and electrons‡. In our case the total number of muons at the observation level is much smaller than the total number of electrons ($N_\mu \simeq 0.03 N_e$; see figure 9). At the same time , at distances $r \geq 1000$ m from the core of the shower inclined at 65°, the muon density ρ_μ exceeds considerably the electron density ρ_e. This effect may have a non-negligible impact on the estimates of the primary energy of inclined electromagnetic showers detected by air shower arrays not identifying the origin of secondary charged particles. At the same time, for the Auger Observatory allowing identification of secondary particles, the detection of unusually high μ/e ratio in inclined showers at large distances from the shower core should not be *a priori* accepted as hadronic showers.

7. Conclusion

The technique of adjoint cascade equations has been applied to study the characteristics of air showers created by EHE γ-rays such as the total numbers of cascade electrons and photoproduced muons at the observation level, the longitudinal and lateral distributions of electrons and muons. Both the LPM effect and interactions of primary γ-rays with the geomagnetic field have been incorporated in the computational code.

The LPM effect changes dramatically the energy dependence of the muon content N_μ. Due to this effect the growth of N_μ with energy gradually disappears producing a local maximum around $E_\gamma \sim 10^{20} - 10^{21}$ eV, after which N_μ decreases with E_γ. The interactions of γ-rays with GMF which start to "operate" almost simultaneously with the LPM effect (i.e. at $E \geq 10^{19}$ eV) recover the nominal energy dependence of N_μ "switching off" the LPM effect.

The ratio of muon contents in the γ-ray and proton induced showers ranges between $0.1 - 0.2$ in the EHE energy region, but decreases significantly at lower energies. The energy dependence of this quantity has a rather complicated (non power-law) form.

Due to the combination of LPM and GMF effects the cascade curves of electrons in γ-ray induced showers are quite similar to these curves for the proton-induced showers. This makes unfortunately rather difficult the separation of γ-induced air showers on the basis of the temporal profiles of the fluorescent light by the Fly's Eye type detectors, except a narrow primary energy band (around 10^{19} eV) and a specific region of arrival

† For the inclined air showers we consider the LDF averaged over the azimuth angle in a plane perpendicular to the shower arrival direction.

‡ For the LDF of electrons we use data from Ref. [44].

directions (depending on the detector location site) for which γ-rays freely pass through the Earth's magnetosphere.

The effect of LPM, when combined with interactions of γ-rays with the GMF, on the lateral distribution of photoproduced muons is quite small. The γ-induced air shower has an essentially narrower lateral distribution of muons compared with the proton shower. This feature can be effectively used for separation of γ-ray induced air showers by the particle detectors of the Auger Observatory. The extension of the muon LDF increases considerably with the zenith angle of arriving primary γ-rays. This results in an interesting effect - the density of muons at large distances from the shower core ($\geq$ 1000 m) may noticeably exceed the electron density.

Acknowledgements

We are grateful to V.Sahakian for valuable discussions.

References

[1] Hillas A M 1984 *Ann. Rev. Astron. Astrophys.* **22** 425
[2] Cesarsky C J 1992 *Nucl. Phys. B* **28B** 51
[3] Rachen J P, Bierman P L 1993 *Astron. Astrophys.* **272** 161
[4] Milgrom M and Usov V 1995 *Ap.J.* **449** L37
[5] Waxman E 1995 *Phys. Rev. Letters* **75** 386
[6] Vietri M 1995 *Ap.J.* **453** 883
[7] Berezinsky V S and Grigor'eva S I 1988 *Astron. Astrophys.* **199** 1
[8] Aharonian F A and Cronin J W 1994 *Phys. Rev. D* **50** 1892
[9] Stanev T, Engel R, Mücke A, Protherpe R, Rachen J 2000 *Phys. Rev. D* **62** 093005
[10] Cronin J 1999 *Rev. Mod. Phys.* **71** S165
[11] Nagano M and Watson A A 2000 *Rev. Mod. Phys.* **72** 2000
[12] Bhattacharjee P and Sigl S 2000 *Physics Reports* **327** 109
[13] Aharonian F A, Bhattacharjee P and Schramm D N 1992 *Phys. Rev. D* **D46** 4188
[14] Berezinsky V S, Kachelriess M, Vilenkin A 1997 *Phys. Rev. Lett.* **79** 4302
[15] Birkel M and Sarkar S 1998 *Astropart. Phys.* **9** 297
[16] Wdowczyk J and Wolfendale A W 1990 *Astrophys.J.* **349** 35
[17] Aharonian F A, Kanevsky B L and Vardanian V V 1990 *Asrophys. Space Sci.* **167** 111
[18] Stanev T and Gaisser T K 1985 *Phys. Rev. D* **32** 1244
[19] Edwards P G, Protheroe R J and Rawinsky E. 1985 *J.Phys.G.*
[20] Hillas A M 1985 *Proc. of 19th ICRC* (La Jolla) **7** 231
[21] Procureur J and Stamenov J N 1987 *J.Phys.G.* **13** 1579
[22] Aharonian F A, Kanevsky B L and Sahakian V A *J.Phys.G.* **17** 1909.
[23] Uchaikin V V and Ryzhov V V 1988 *Stochastic theory of transport of high energy particles* (Novosibirsk, Nauka) (in Russian)
[24] Landau L D and Pomeranchuk I J 1953 *Dokl. Akad. Nauk SSSR* **92** 535
[25] Migdal A B 1956 *Phys. Rev.* **103** 1811

[26] McBreen B and Lambert C J 1981 *Phys. Rev. D* **24** 2536
[27] Goncharov A I 1991 *PHD thesis* Tomsk Technical University (in Russian)
[28] Halzen F, Vasques R, Stanev T, Vankov H P 1995 *Astropart. Phys.* **3** 151
[29] Kasahara K 1996 In: *Extremely High Energy Cosmic Rays: Astrophysics and Future Observations* (Tokyo, ed. by M.Nagano) 221
[30] Bertou X, Billoir P, and Dagoret-Campagne S. 2000 *Astropart. Phys.* **14** 121
[31] Capdevielle J N, Le Gall C and Sanosyan Kh N 2000 *Astropart. Phys.* **13** 277
[32] Angelov V and Vankov H 1999 *J.Phys.G.* **25** 1755
[33] Akhiezer A I, Merenkov N P and Rekalo A P 1994 *J.Phys.G.* **20** 1499
[34] Chapman S and Bartels J 1940 *Geomagnetism v.1-2* (Oxford University Press London&New-York)
[35] The Auger Observatory Design Report: httm://www.auger.org
[36] Cillis A and Sciutto S 2000 *J.Phys.G.* **26** 309
[37] Webpage *www.ngdc.noaa.gov*
[38] Muecke A, Engel R et al 2000 *Comp. Phys. Comm.* **124** 290
[39] Shabelsky Yu M 1986 *Yadernaia Fizika* **44** 186 (in Russian)
[40] Shabelsky Yu M 1987 *Yadernaia Fizika* **45** 223 (in Russian)
[41] Kolchuzhkin A M and Plyasheshnikov A V 1975 *Atomnaia Energia* **38** 327 (in Russian)
[42] Plyasheshnikov A V, Lagutin A A and Uchaikin V V 1979 *Proc. of 16-th ICRC* (Kyoto) **7** 1
[43] McComb T J *et al* 1979 *J.Phys.G.* **5** 1613
[44] Lagutin A A, Plyasheshnikov A V *et al* 1999 *Izvestia AGU. Special Issue* (Barnaul, Russia) 33
[45] Heck D, Knapp J *et al* 1998 *Forschungzentrum Karlsruhe Report FZKA 6019*
[46] Hillas A M 1985 *Proc. of 19th ICRC* (La Jolla) **1** 155
[47] Nagano M, Heck D *et al* 2000 *Astropart.Phys.* **13** 277
[48] Danilova T V, Erlykin A D *et al* 1985 *Proc. of 19th ICRC* (La Jolla) **7** 260
[49] Chatelet E, Procureur J *et al* 1990 *J.Phys.G* **16** 317
[50] Sciutto S G 1999 *Preprint astro-ph/9911331*
[51] Ave M, Hinton J A *et al* 2000 *Preprint astro-ph/0007386*
[52] Dedenko L G 1987 *Proc. of 20th ICRC* (Moscow) **6** 154
[53] Plyasheshnikov A V, Aharonian F A *et al* 1998 *J.Phys.G.* **24** 653

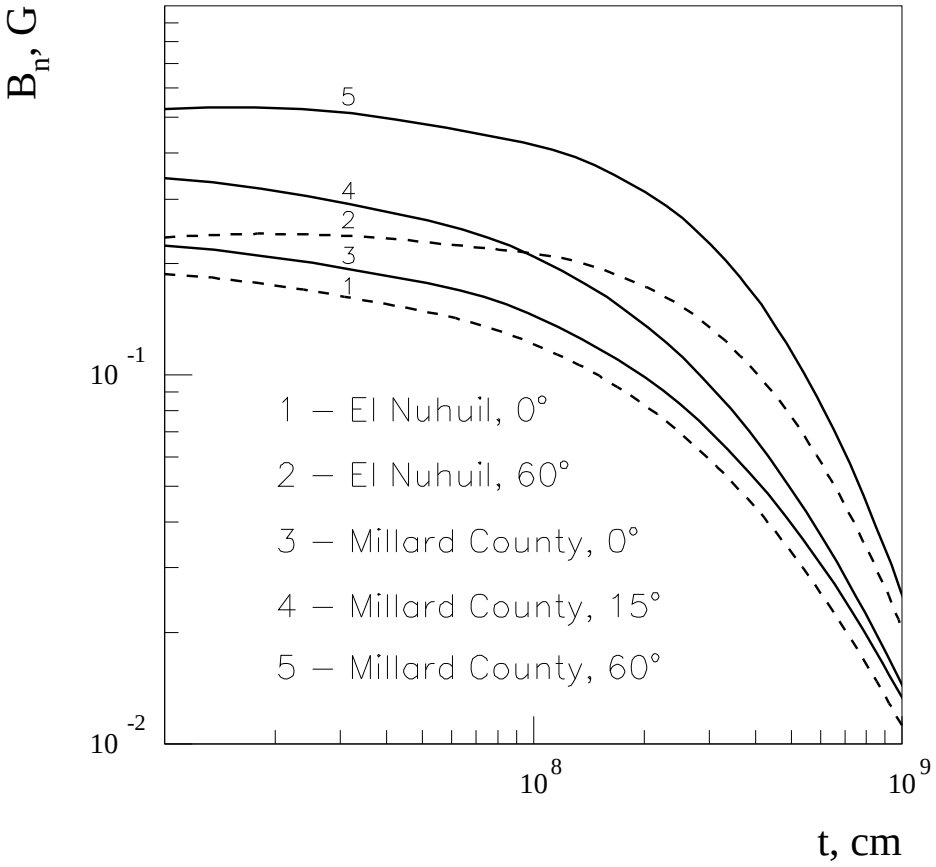

Figure 1. Profiles of the perpendicular component of geomagnetic field for different detector locations and for different zenith angles of arriving γ-ray photon.

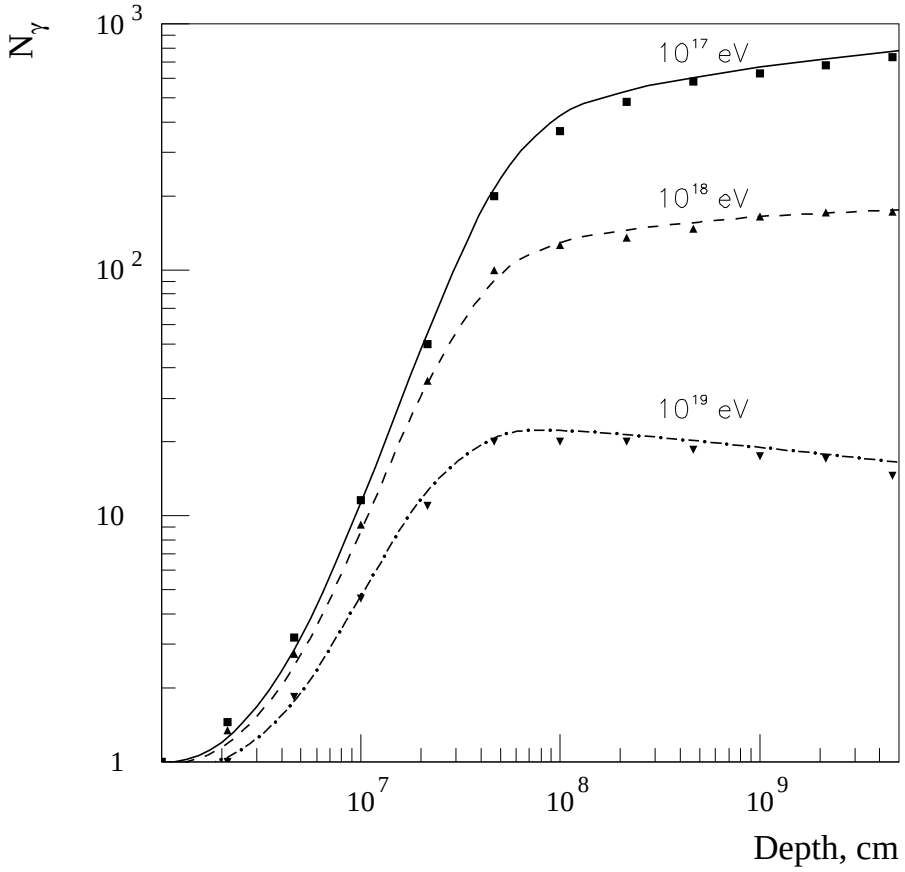

Figure 2. The number of secondary synchrotron photons with energies $E \geq 10^{17}$, 10^{18} and 10^{19} eV produced in the homogeneous magnetic field with $B_{\rm n} = 0.3$ G by primary γ-rays of energy 10^{21} eV. Curves – this work; points – from Ref. [27].

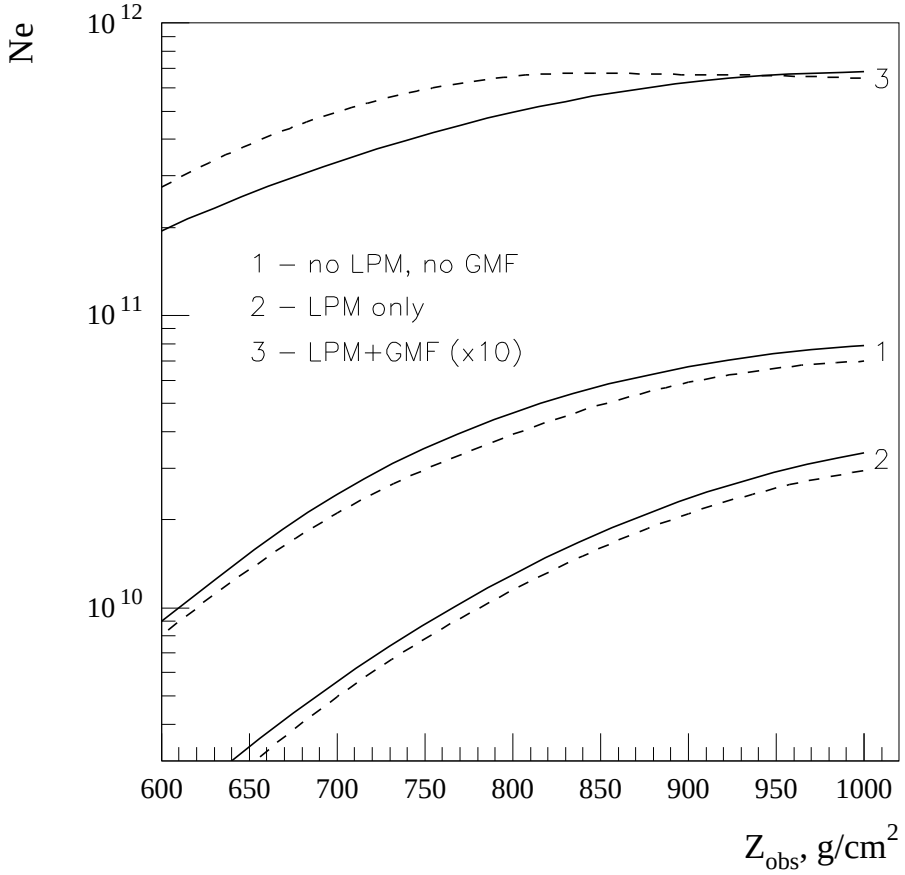

Figure 3. Dependence of the number of cascade electrons with energy $T \geq 0$ on the depth of the observation level for vertical primary γ-rays of energy 10^{20}eV with use of different assumptions concerning the LPM and GMF effects. Solid curves – this work; dashed curves – from Ref. [22].

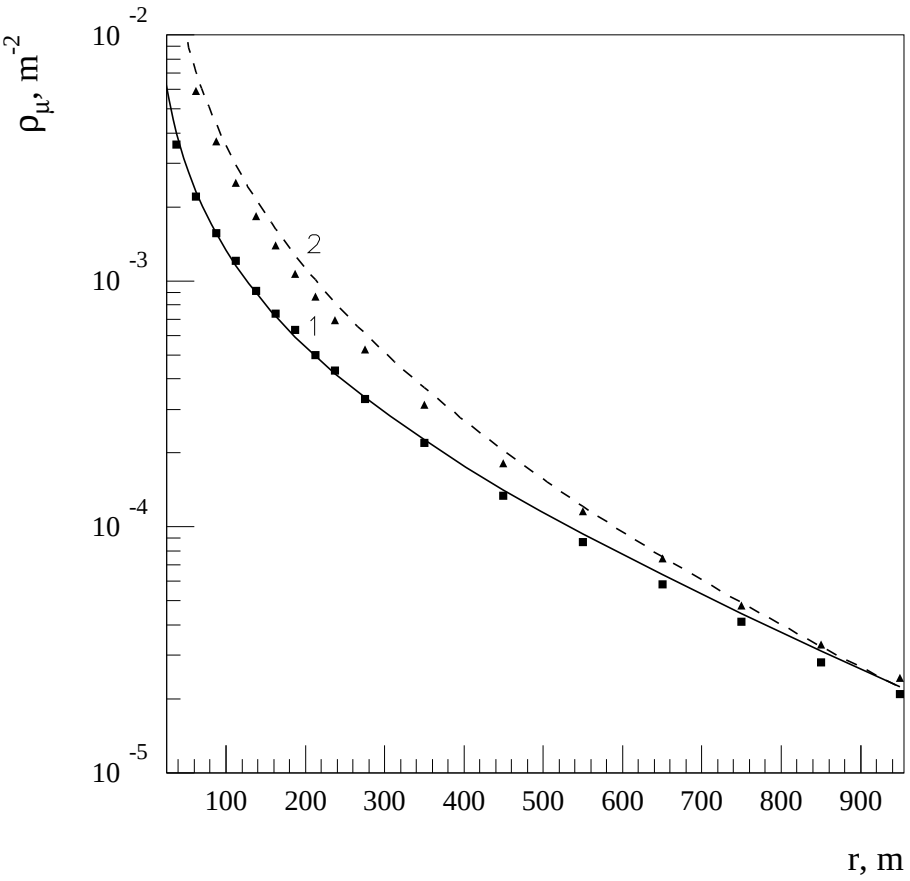

Figure 4. The radial dependence of the density of muons with energy $T \geq 0$ for vertical air showers produced by primary γ-rays with energy $E = 10^{15}$ eV at the sea level (1) and at 5 km above the sea level (2). Curves – numerical solution of adjoint equations; points – simulations with CORSIKA.

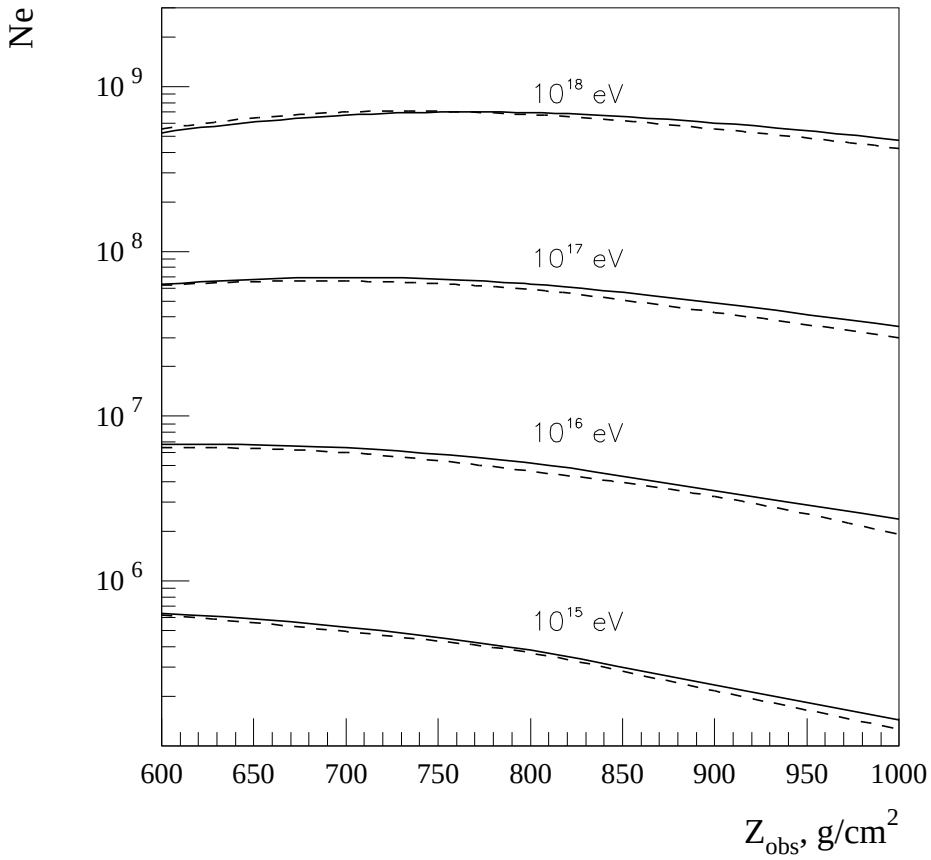

Figure 5. The number of electrons with energy $T \geq 0$ in the air showers initiated by vertical protons as a function of the penetration depth. The energies of primary protons are indicated at the curves. Solid curves – present work; dashed curves – from Ref. [44].

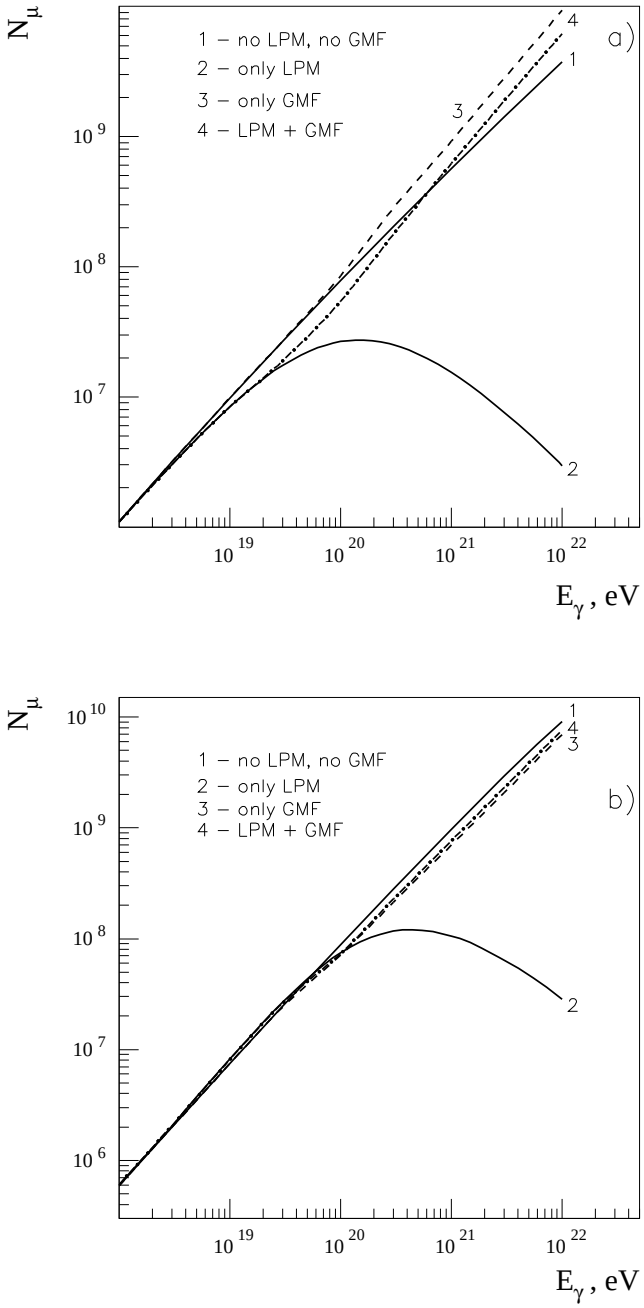

Figure 6. Dependence of the number of muons with energy $T \geq 0$ on the energy of primary γ-ray for different assumptions concerning the LPM and GMF effects calculated for the El Nuhuil site. Vertical (a) and inclined (b, 45°) showers are considered.

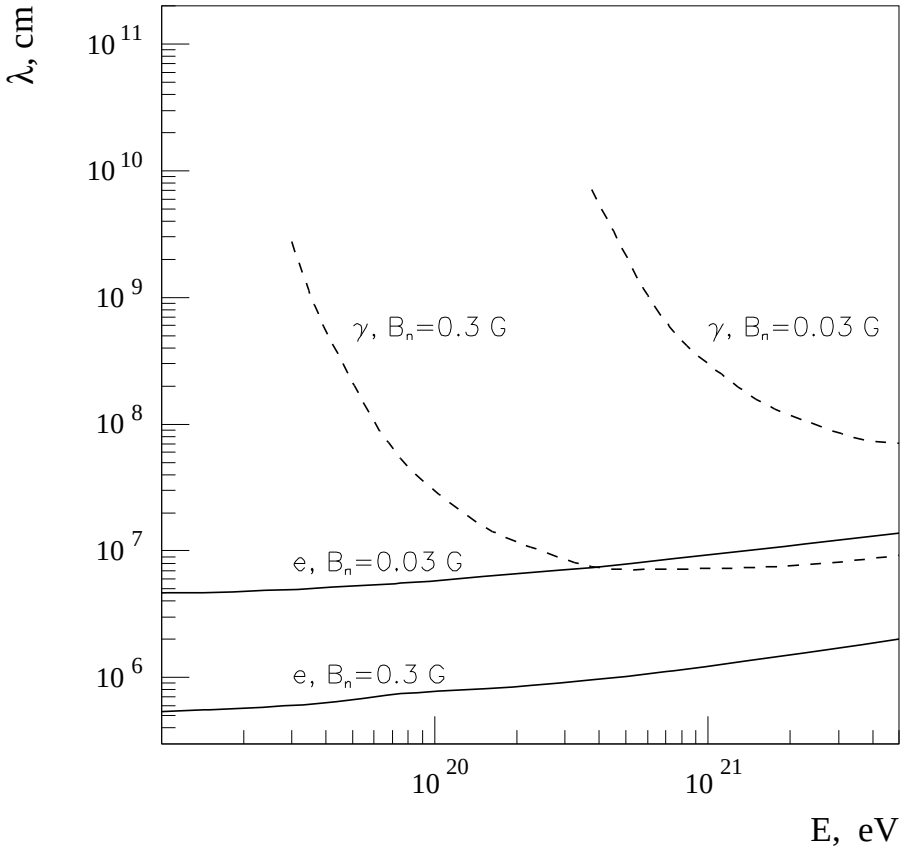

Figure 7. The energy dependence of the mean free pathlength of γ-rays and electrons in the homogeneous magnetic field $B_{\rm n} = 0.3$ and 0.03 G.

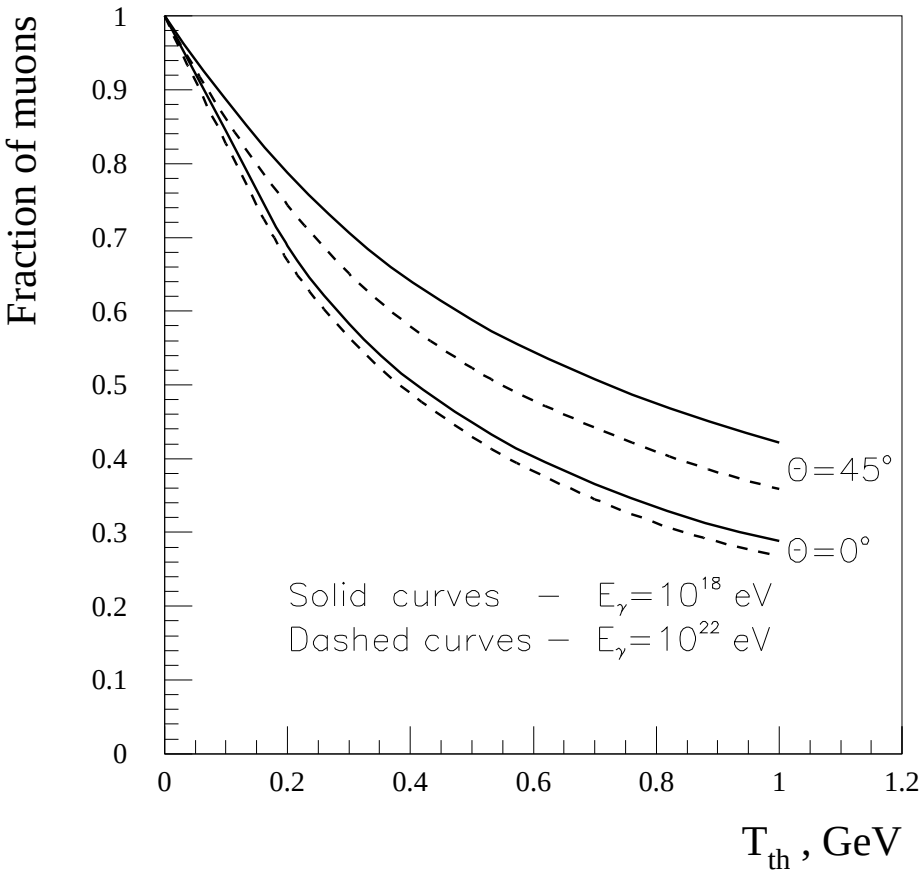

Figure 8. The fraction of muons with kinetic energy larger than T_{th} for different incident angles θ and energies E_γ of primary γ-ray. The El Nuhuil site.

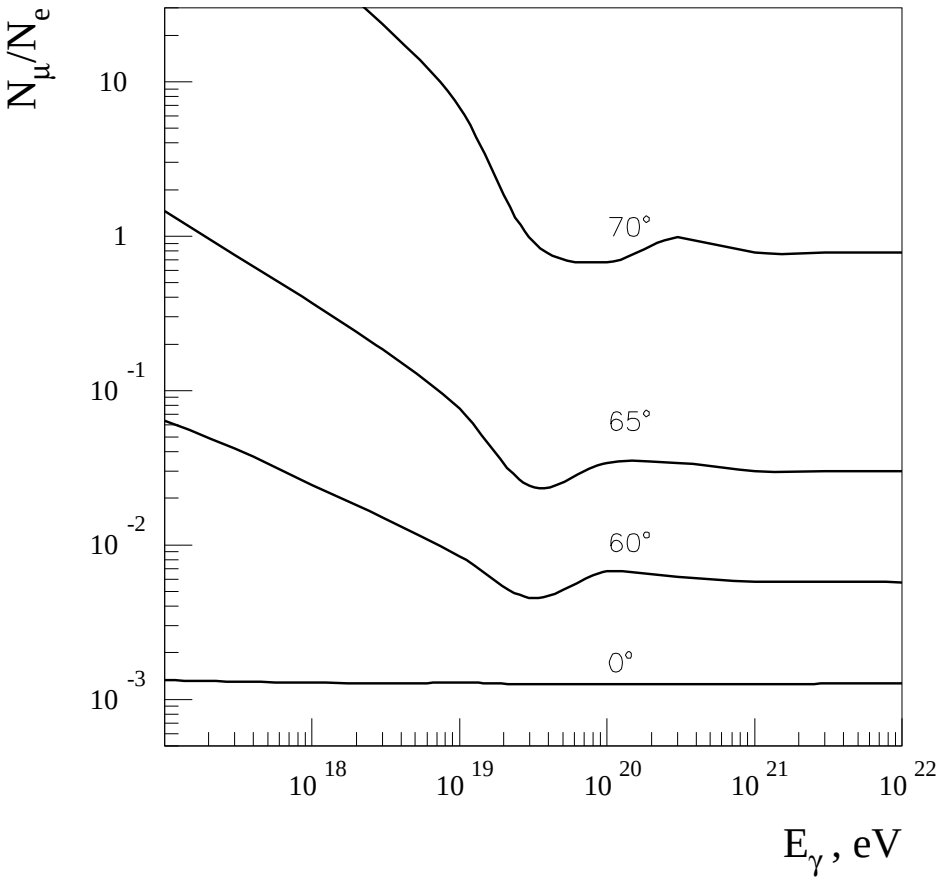

Figure 9. The ratio of total numbers of muons and electrons as a function of energy of primary γ-ray. The zenith angles of the arriving γ-rays are indicated at the curves. The El Nuhuil site.

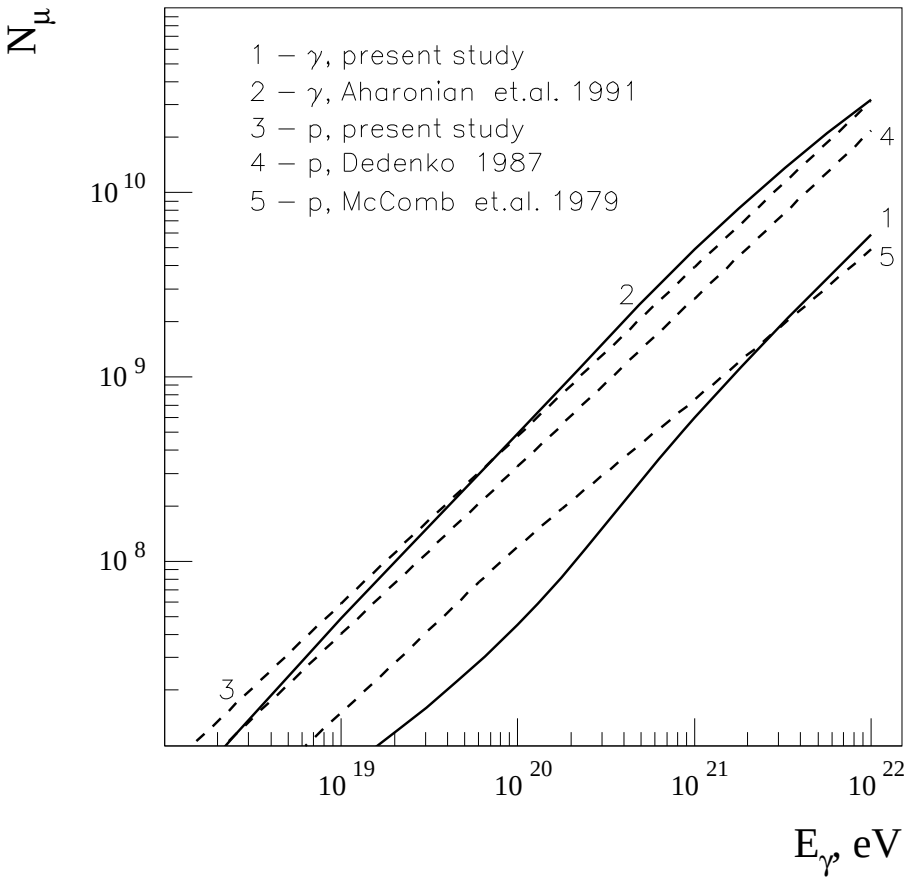

Figure 10. The energy dependence of number of muons with total energy $E_{th} \geq 0.3$ GeV for vertical γ-ray and proton induced showers at the sea level.

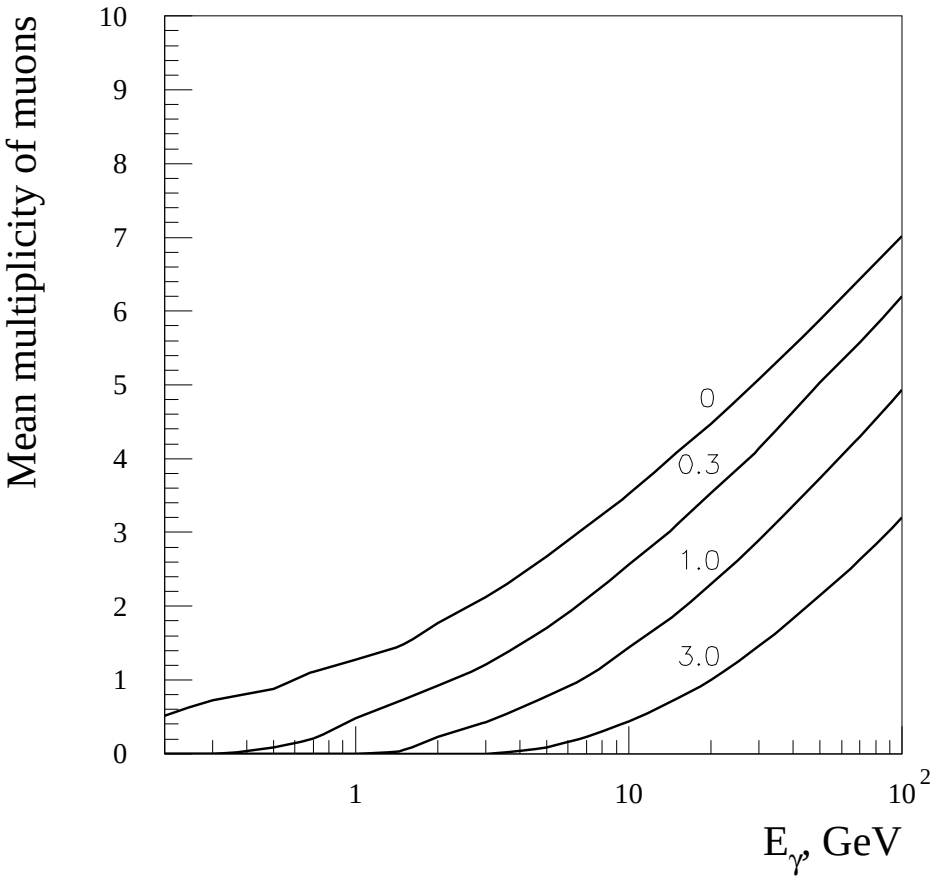

Figure 11. The mean multiplicity of muons with kinetic energy $T \geq T_{\rm th}$ produced in the γ-nuclear interactions as a function of the γ-ray energy. The values of $T_{\rm th}$ are indicated at the figures.

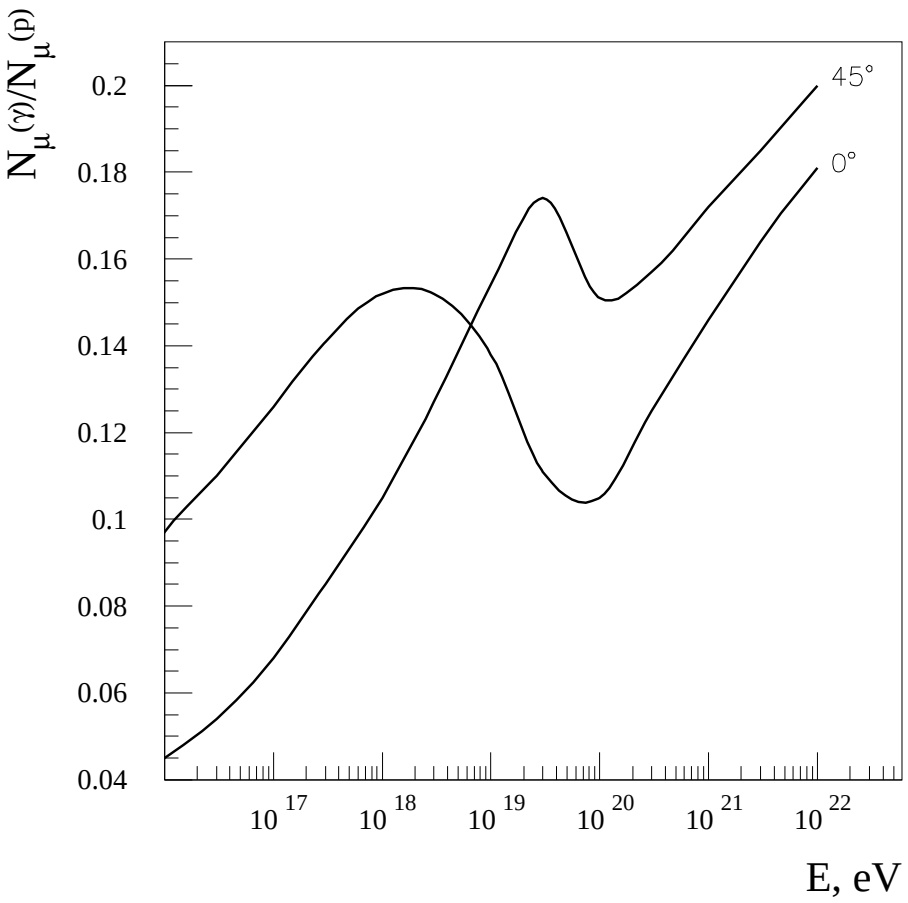

Figure 12. The ratio of the contents of muons with energy $T \geq 0$ for air showers produced by primary γ-rays and protons. The arrival angles of primary particles are indicated at the curves. The El Nuhuil site.

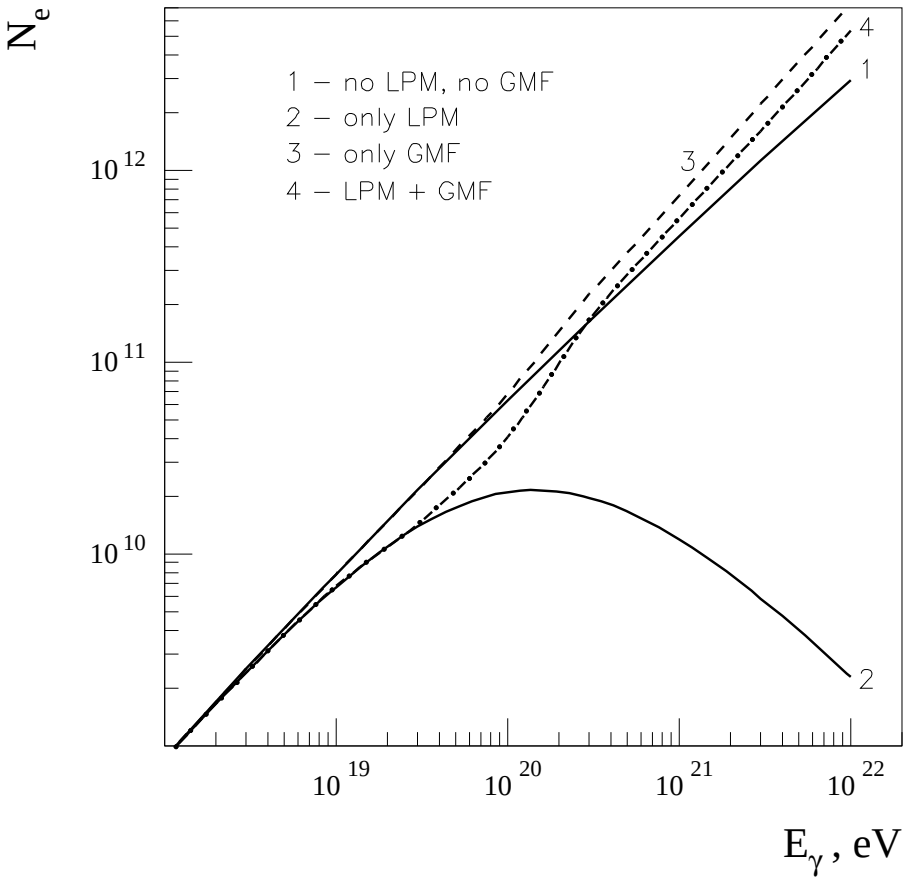

Figure 13. Dependence of the number of cascade electrons with energy $T \geq 0$ on the energy of vertical γ-ray and proton induced air showers for different assumptions concerning the LPM and GMF effects. The El Nuhuil site.

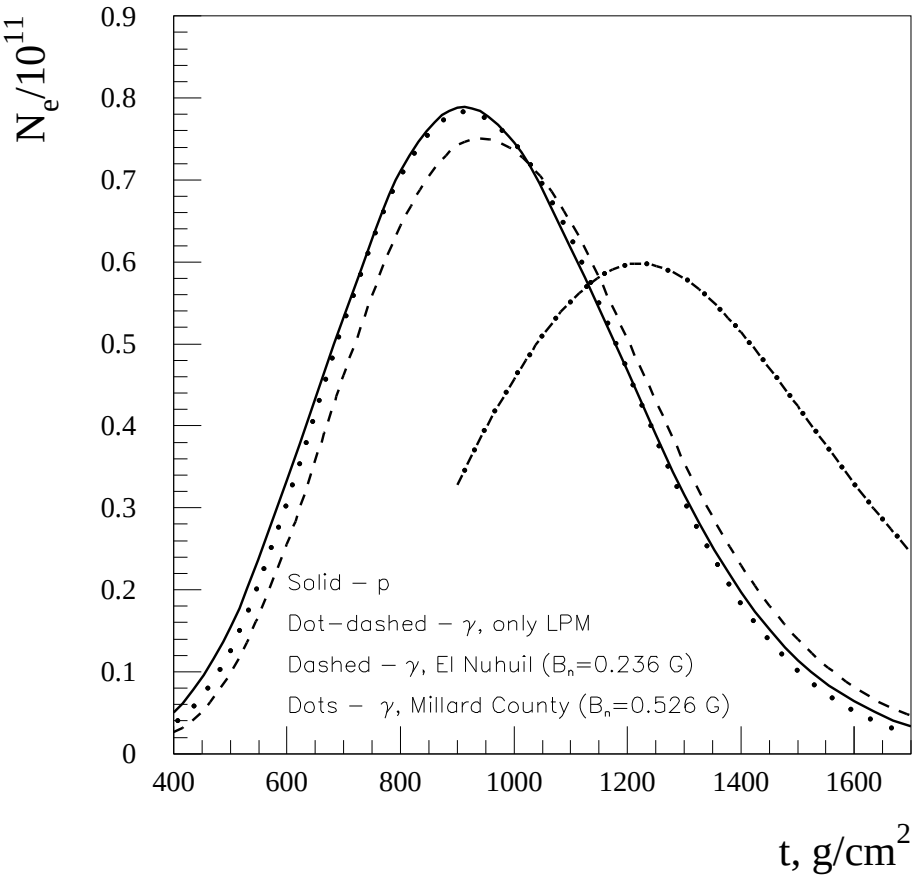

Figure 14. The number of cascade electrons with energy $T \geq 0$ as a function of the penetration depth for primary protons and γ-rays of energy 10^{20} eV. Two different detector locations – El Nuhuil and Millard County – are considered for inclined (60°) air showers.

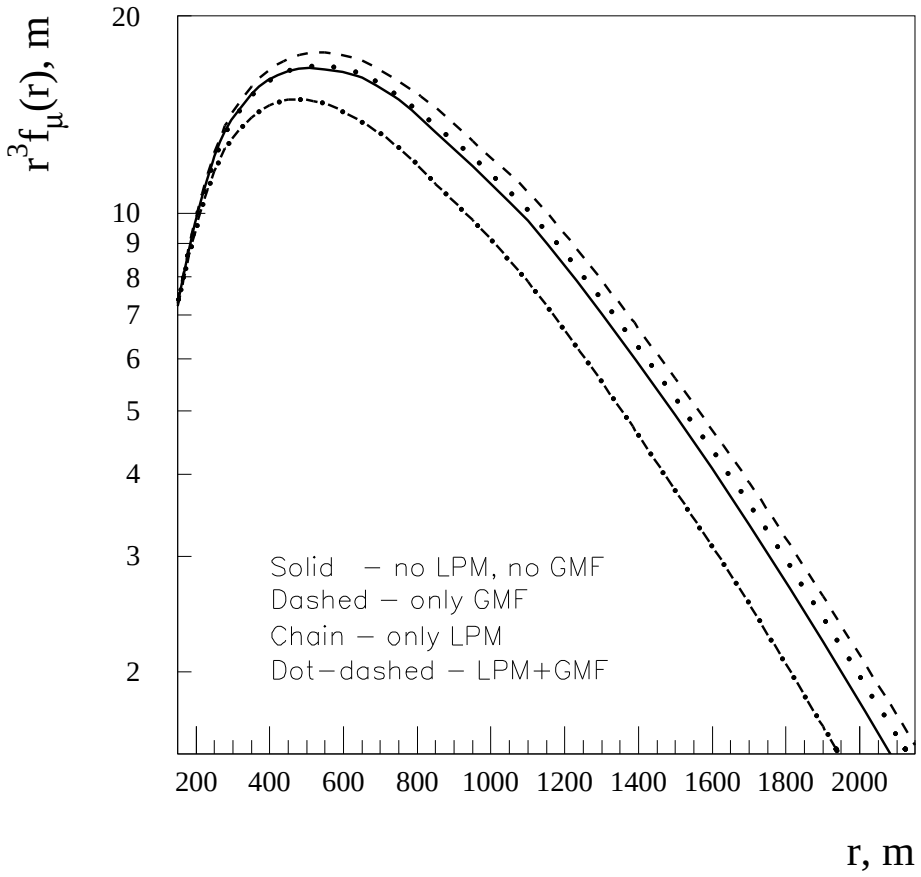

Figure 15. The lateral distributions of muons with energy $T \geq 0$ for vertical showers induced by a primary γ-ray of energy 10^{20} eV, calculated for different assumptions concerning the LPM and GMF effects. The El Nuhuil site.

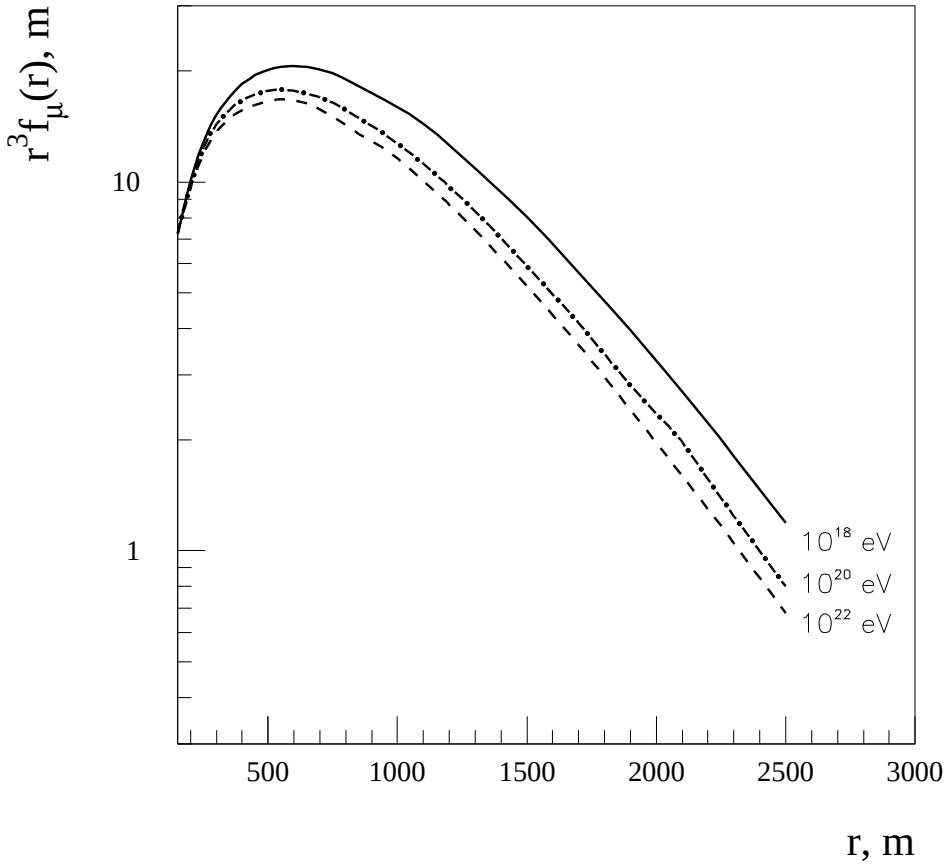

Figure 16. The lateral distributions of muons with energy $T \geq 0$ for vertical γ-ray showers of energies indicated at the curves. The El Nuhuil site.

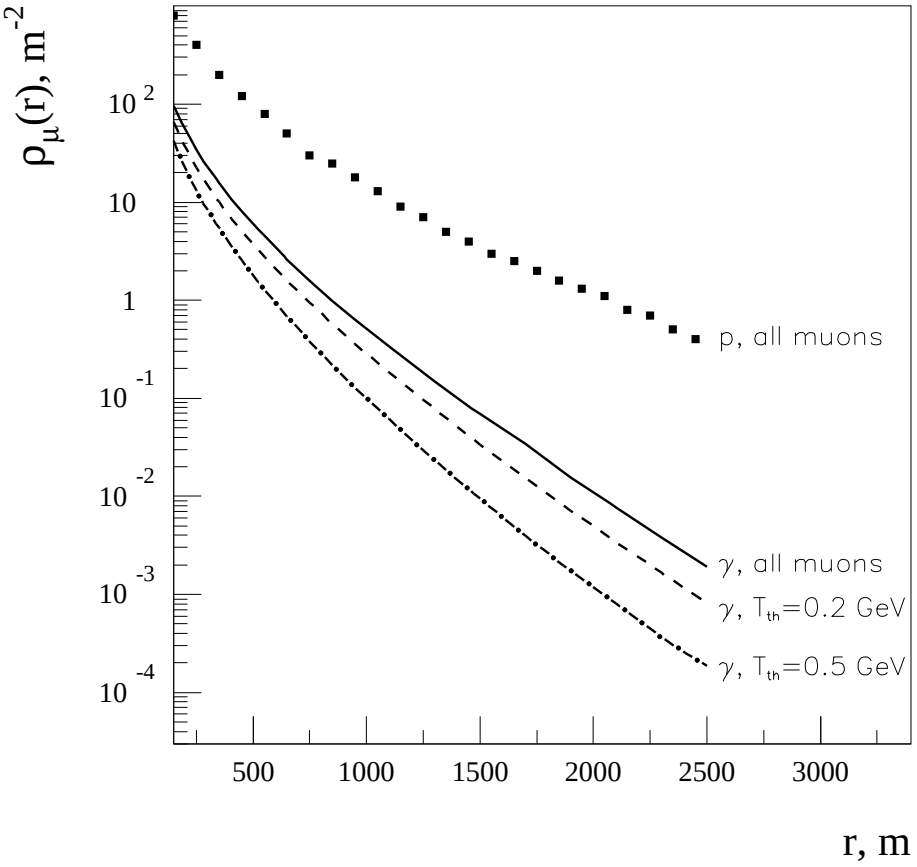

Figure 17. The muon density in the vertical showers produced by protons and γ-rays of energy 10^{20} eV. The results of present work for primary γ-ray (the El Nuhuil site) and for three different muon threshold energies are compared with results of Ref. [47] calculated for primary protons at $Z_{\rm obs} = 920$ g/cm^2 .

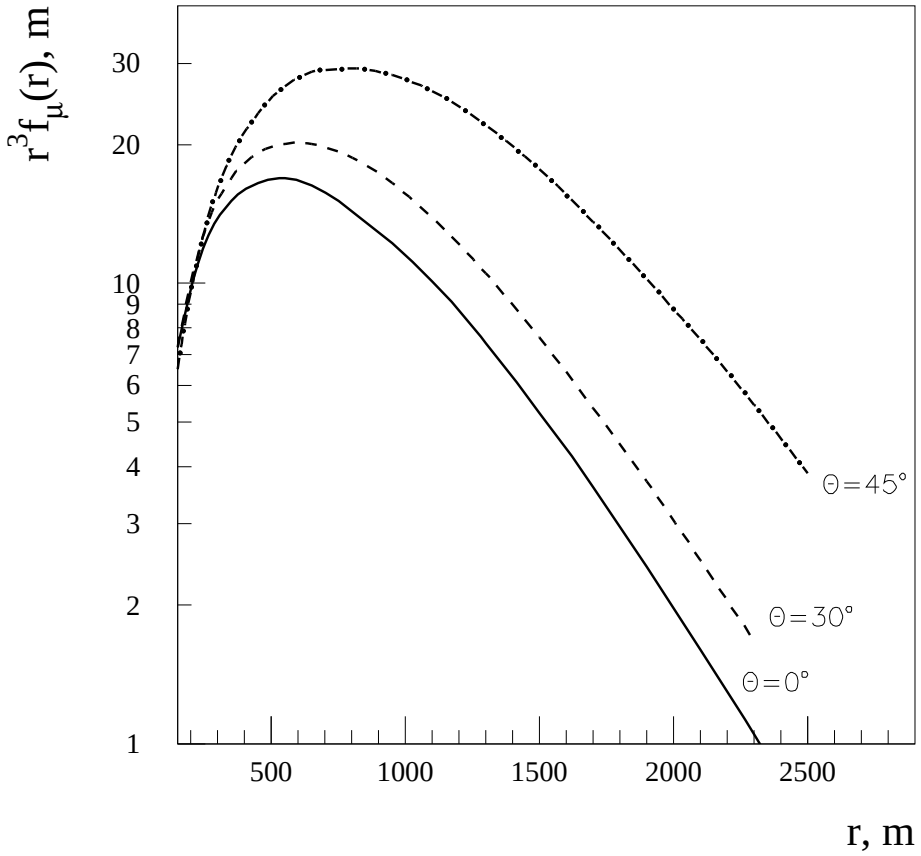

Figure 18. The lateral distributions of muons with energy $T \geq 0$ in the electromagnetic showers for 3 different arrival angles of primary γ-ray of energy 10^{20} eV. The El Nuhuil site.

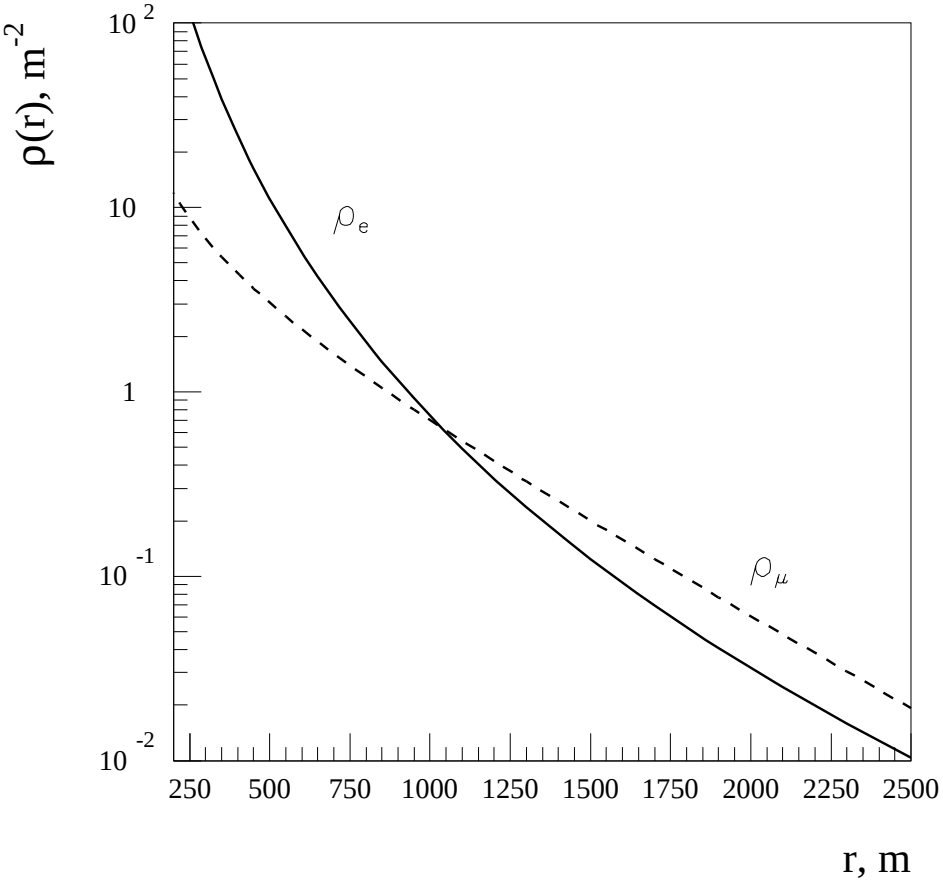

Figure 19. The densities of muons (ρ_μ) and electrons (ρ_e) in the inclined (65°) γ-ray shower of energy 10^{20} eV. The El Nuhuil site.